NANO LETTERS

2007
Vol. 7, No. 8
2322−2327

Nanocrystal-Encoded Fluorescent Microbeads for Proteomics: Antibody Profiling and Diagnostics of Autoimmune Diseases

Alyona Sukhanova,[†] Andrei S. Susha,[‡] Alpan Bek,[‡] Sergiy Mayilo,[‡] Andrey L. Rogach,*[,‡] Jochen Feldmann,[‡] Vladimir Oleinikov,[†] Brigitte Reveil,[†] Beatrice Donvito,[†] Jacques H. M. Cohen,[†] and Igor Nabiev*[,†]

EA No. 3798 Détection et Approches Thérapeutiques Nanotechnologiques dans les Mécanismes Biologiques de Défense, Université de Reims Champagne-Ardenne, 51100 Reims, France, and Department of Physics and Center for NanoScience (CeNS), Ludwig-Maximilians-Universität München, 80799 Munich, Germany

Received April 24, 2007; Revised Manuscript Received July 11, 2007

ABSTRACT

The first application of nanocrystal (NC)-encoded microbeads to clinical proteomics is demonstrated by multiplexed detection of circulating autoantibodies, markers of systemic sclerosis. Two-color complexes, consisting of NC-encoded, antigen-covered beads, anti-antigen antibody or clinical serum samples, and dye-tagged detecting antibodies, were observed using flow cytometry assays and on the surface of single beads. The results of flow cytometry assays correlated with the ELISA technique and provided clear discrimination between the sera samples of healthy donors and patients with autoimmune disease. Microbead fluorescence signals exhibited narrow distribution regardless of their surface antigen staining, without the need of any fluorescence compensation—a parameter determining the limit of sensitivity of flow cytometry assays. In single bead measurements, less than 30 dye-labeled antibodies interacting with the topol-specific antibodies at the surface of a bead have been detected by the emission of dye excited through the FRET from NCs. In this format, the antibody–bead interaction reaction turns specifically the fluorescence signal from dye label off and on, additionally increasing autoantibody detection sensitivity.

Many human diseases are the result of autoimmune attack, presumably related to a loss of tolerance to self. Notwithstanding the underlying mechanism of autoimmune disease, virtually all of them are associated with circulating autoantibodies, which bind self-proteins. The scleroderma (systemic sclerosis) autoimmune diseases are associated with presence of antinuclear antibodies such as anti-Scl-70, anti(nuclear ribonucleoprotein, nRNP), anti(Sm-antigen), and some other autoantibodies.[1] They are of diagnostic value and are reported as being present or absent determining diagnosis of affected patients and their prognosis.[1] The antigen of anti-Scl-70 antibody (also called anti-topoI antibody) is human DNA-topoisomerase I (topoI).[2,3] The "gold standard" method for detection of circulating autoantibodies is the indirect immunofluorescence (IIF) assay.[4] Considerable effort has been made in developing alternative automated and more sensitive diagnostics for routine laboratory use, since IIF assays are time-consuming and their standardization is difficult due to the subjective interpretation.[5] Immunoassay-based ELISA methods[6] and microbeads-based flow cytometry technology employing organic dyes as fluorescent tags[7] present the advantage of rapidity, objectivity, and ability of automation.

Bead-based assays on very large numbers of molecules require encoding of each of the microbeads according to the particular ligand bound to its surface.[8,9] Polymeric beads optically encoded with organic dyes allow for a limited number of unique codes[10−12] whereas the use of semiconductor nanocrystals (NCs) as fluorescent tags improves the beads multiplexing capabilities, photostability, and sensitivity of the antigen detection.[13−15] Fluorescent NCs provide unique advantages over organic dyes in high-throughput screening, including high brightness and resistance to photobleaching. NC broad absorption spectra ensure excitation of various populations of NCs (each having a narrow emission spectrum determined by their size and chemical composition) using a single wavelength far removed from their respective emission, thus avoiding spectral overlap and improving multiplexing capability. The use of NCs as FRET donors sensitive to molecular binding events utilizes strongly absorbing NCs

* To whom correspondence should be addressed. E-mails: andrey.rogach@physik.uni-muenchen.de (A.L.R.), igor.nabiev@univ-reims.fr (I.N.).
† Université de Reims Champagne-Ardenne.
‡ Ludwig-Maximilians-Universität.

10.1021/nl070966+ CCC: $37.00
Published on Web 07/24/2007

for focusing incident light on a weakly absorbing organic dye via energy transfer,[16] where emission of NC donor can be size-tuned to improve the spectral overlap with a particular dye acceptor.

A first proof-of-concept publication proposed to use NC-encoded microbeads for multiplexed detection of oligonucleotide probes hybridization.[13] Follow-up studies validated the NC-tagged microbeads as a sensitive tool for high-throughput genotyping of single nucleotide polymorphisms[14] and for gene expression profiling.[15] Despite these examples of genomic applications, the potential of NC-encoded microbeads in clinical proteomics remains to be demonstrated.

In this Letter, we demonstrate the first application of NC-encoded microbeads to proteomics, for multiplexed antibody profiling and clinical diagnostics of autoimmune diseases. Latex microbeads were optically encoded with NCs of different colors, coated with recombinant 68 kDa fragment of topoI, nRNP, or Sm-antigen, and applied to detection of corresponding circulating autoantibodies, markers of systemic sclerosis. Two-color complexes, consisting of NC-encoded antigen-covered beads, anti-antigen antibody or clinical serum samples, and dye-tagged detecting antibodies, were observed using flow cytometry assays and on the surface of single beads.

Preparation of NC-encoded microbeads suitable for immunodiagnostics of autoimmune diseases included (i) synthesis[17] and functional water-solubilization of CdSe/ZnS core/shell NCs[18] of different sizes (colors of emission), (ii) preparation, by the method of layer-by-layer electrostatic deposition of polymers[19] in combination with infiltration of NCs,[20] of optically encoded homogeneous and brightly fluorescent microbeads, and (iii) expression and purification of enzymatically active 68 kDa recombinant fragment of human topoI (see Supporting Information). Extracts for autoimmune testing, including Sm-antigen and nRNP complex (calf thymus origin) were purchased from ImmunoVision. For studies reported in our paper, CdSe/ZnS NCs emitting in green (530 or 545 nm), orange (570 or 590 nm), or red (630 nm) with a quantum yield of 40% in aqueous solutions were embedded into presurface layer of polymer-coated monodispersed melamine formaldehyde latex microbeads of 3 μm diameter (panels a and b of Figure 1). The surfaces of NC-encoded microbeads of different colors were rendered specific to autoantibodies by passive adsorption on their surfaces of corresponding antigens: 68 kDa fragment of topoI, nRNP or Sm-antigen. The NC-encoded and antigen-covered microbeads were finally back-coated with bovine serum albumin (BSA) protein.

The principle of flow cytometry assay used is shown in Figure 1c. Flow cytometry analysis demonstrated that the NC-encoded topoI-covered microbeads were extremely bright and homogeneous (Figure 2a). In order to confirm the presence of topoI at the microbead's surface, they were incubated with the monoclonal anti-topoI antibodies and stained by the FITC-labeled goat F(ab′)2 fragment of anti-mouse immunoglobulin (IgG). Figure 2b demonstrates the shift of fluorescence signal from orange (fluorescence from the NCs on microbeads) to green area (signal from the FITC)

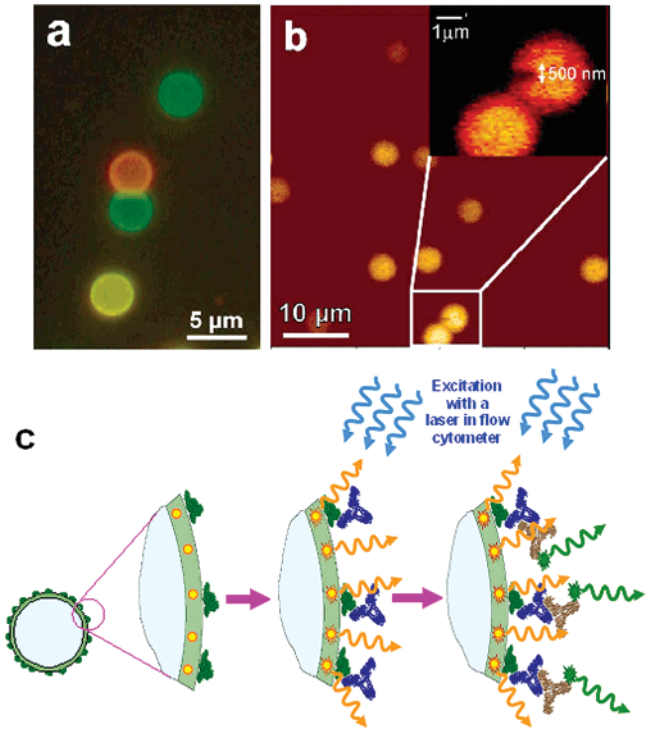

Figure 1. Nanocrystal-encoded, antigen-coated microbeads for diagnostics of autoimmune diseases. (a) Fluorescence micrograph of a mixture of microbeads encoded with NCs of different emission colors. (b) Fluorescence image of NC-encoded beads obtained with a confocal laser scanning optical microscope. Insert demonstrates the spot size of the excitation beam on the surface of a NC-encoded microbead intentionally photobleached by high-power laser illumination. (c) Scheme of a flow cytometry assay for immunodetection of autoantibodies, markers of systemic sclerosis, with NC-encoded, antigen-coated microbeads. Here, microbeads optically encoded with orange-emitting NCs and coated by 68 kDa recombinant fragment of human DNA topoisomerase I (topoI) are incubated with anti-topoI specific monoclonal antibodies or with the serum samples of patients and stained with green-emitting FITC-labeled secondary antibodies. Excitation is provided by the 488 nm line of an Ar laser.

after addition of FITC-labeled IgG, clearly approving the presence of topoI at the microbead's surface. The negative controls included incubation of microbeads with a nonspecific analyte (anti-CD3 antibody, Figure 2c) or with the FITC-labeled goat F(ab′)2 fragment of IgG in the absence of specific anti-topoI antibody (Figure 2d) where no fluorescence shift has been detected. Quantitative statistical data based on analysis of the positive and negative events in these experiments show an existing clear discriminative criteria of anti-topoI antibodies binding (Table I, Supporting Information). NC-encoded bead light scattering (left columns of Figure 2) and fluorescence signals exhibited a very narrow distribution peak, regardless of their surface antigen staining, particularly without any need of fluorescence compensation. For example, 90% of all the topoI-covered beads were found to be within 71 out of 10 000 detector channels whereas 88% of beads with two-color immunocomplexes on their surfaces are within the 67 out of 10 000, corresponding to microbead heterogeneity coefficients 0.007889 and 0.007614, respectively.

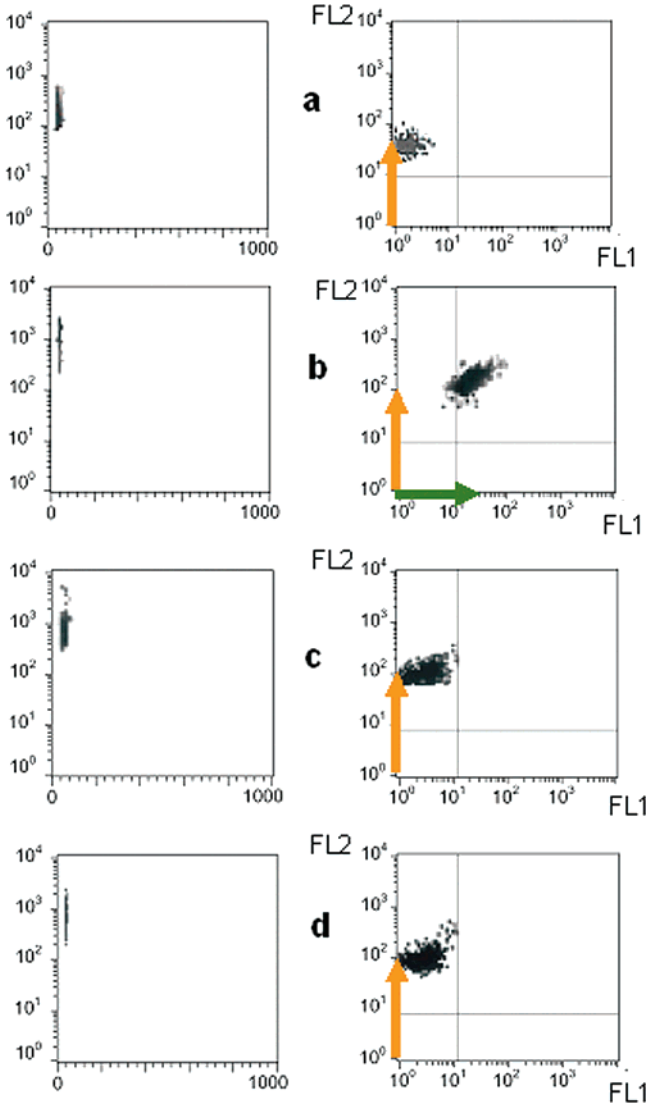

Figure 2. Flow cytometry dot plots of nanocrystal-encoded, topoisomerase I-coated microbeads used for detection of anti-topoisomerase I antibodies (according to schematics of Figure 1c): left column, light scattering measurements; right column, green (FL1) vs orange (FL2) fluorescence profiles. (a) NC-encoded, topoI-coated microbeads. (b) NC-encoded, topoI-coated microbeads incubated with the anti-topoI specific monoclonal antibodies and stained with the FITC-labeled secondary antibodies. (c) Negative control: NC-encoded, topoI-coated microbeads incubated with the anti-CD3 topoI-nonspecific monoclonal antibodies and stained with the FITC-labeled secondary antibodies. (d) Negative control: NC-tagged topoI-coated microbeads incubated with the FITC-labeled secondary antibodies in the absence of primary monoclonal antibodies.

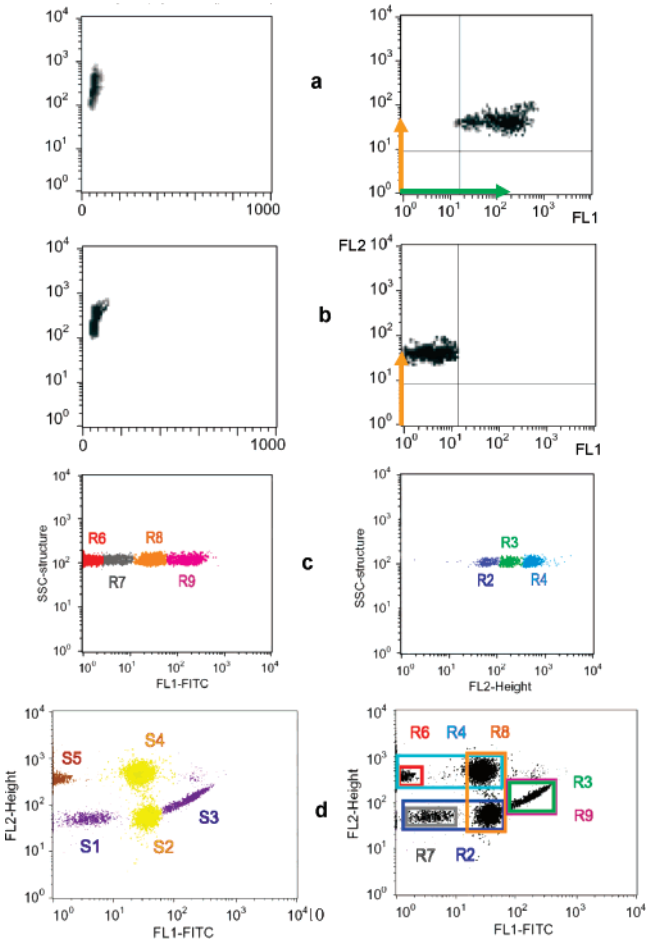

Figure 3. Flow cytometry dot plots of nanocrystal-encoded, antigen-coated microbeads used for detection of autoantibodies, markers of systemic sclerosis, in the clinical serum of healthy donors and patients with systemic sclerosis (according to schematics of Figure 1c). (a, b) Left column, light scattering measurements; right column, green (FL1) vs orange (FL2) fluorescence profiles. Right column: NC-encoded, topoI-coated microbeads incubated in serum of a healthy donor (a) or in serum of a patient with systemic sclerosis (b) and stained with the FITC-labeled secondary antibodies. (c, d) Region windows (R2-R4, R6-R9) and dot plots of a mixture of microbeads encoded with the green (530 nm, S2, S4) or orange (570 nm, S1, S3) or deep-orange (590 nm, S5) NCs and covered with topoI (S1, S3), Sm-antigen (S2, S4), or BSA (S5). Microbeads were incubated in the serum of a healthy donor (S1, S2, S5) or in the sera of patients with an elevated level of anti-Scl-70 (S3) or anti-Sm (S4) autoantibodies. Microbeads were finally stained with the FITC-labeled (S1, S3, S5) or phycoerythrin-labeled (S2, S4) secondary antibodies. Right column in (d) shows relationships between the region windows and signals position in the dot plot.

Thus far, NC-encoded topoI-covered microbeads were proved to be useful for clinical immunodiagnostics of anti-Scl-70 antibodies, markers of systemic sclerosis, in the serum of scleroderma patients. For functional clinical tests we have used the samples of serum from scleroderma disease patients with confirmed elevated level of anti-Scl-70 antibodies and compared them with healthy controls. The sera used were characterized by standard IIF and ELISA techniques (Supporting Information) in order to correlate their results with flow cytometry assay utilizing NC-encoded microbeads. Appearance of fluorescence shift from the orange to green area after incubation of topoI-covered beads with serum of positive patients (Figure 3b) compared with serum of negative patients (Figure 3a) provided a clear discrimination criteria (Table I, Supporting Information) and excellently agreed with the results of traditional IIF and ELISA detection techniques (Supporting Information).

We have further demonstrated in a proof-of-the-principle flow cytometry experiment the first multiplexed detection of different autoantibodies within the sera with elevated level of anti-Scl-70 or anti-Sm autoantibodies using the microbeads encoded with NCs emitting in green and orange regions of

optical spectrum (Figure 3c,d). Here, beads S3 (covered with topoI) and S4 (covered with Sm-antigen) incubated in the sera with elevated level of corresponding autoantibodies provide a clearly positive reaction when compared with the same beads incubated in the sera taken from the healthy volunteers (S1 and S2, respectively). Signals from S3 and S4 slightly differ from an orthogonal representation due to the fluorescence leakage of organic fluorochromes (FITC and, at a less extent, phycoerythrin (PE)), although the signals from NC labels, due to their narrow emission peaks, do not need fluorescence compensation. The compensation requirements in multiplexed flow cytometry assays with fluorescent microbeads encoded with organic dyes impose a strong limit on their sensitivity. Fluorescence spectra of NC-encoded beads are narrow, symmetrical, and do not trail toward longer wavelengths. These advantages of NCs over organic dyes permitted us to record the multiplexed spectra without any fluorescence compensation (Figure 3c,d) ensuring maximal discrimination of multiple signals, thus increasing additionally a sensitivity of multiplexed flow cytometry assays.

The fluorescence emission intensities from microbeads S1 (570 nm) and S2 (530 nm) are not discriminated in the instrument settings chosen for FL2 for the sake of clarity of the demonstration of organic fluorochrome staining discrimination from NCs fluorescence.

To further demonstrate the possibility of antibody ultrasensitive screening and to estimate the limit of autoantibody detection with NC-encoded microbeads, we have employed a single-bead immunodiagnostics format relying on FRET between NCs and dye molecules labels of a secondary antibody (Figure 4a). Microbeads encoded with orange-emitting NCs and coated by a 68 kDa fragment of topoI were incubated with the anti-topoI specific antibodies and stained with the AlexaFluor633-labeled secondary antibodies. In the single-bead setup, a confocal laser scanning optical microscope was equipped with a laser generating light at 532 nm and with a lamp providing a broad-band excitation between 450 and 500 nm (Supporting Information). As shown in Figure 4b, AlexaFluor633 dye used as a label for secondary antibody does not absorb light at wavelengths lower than 500 nm and cannot be excited by the lamp, whereas the NCs can be excited by both light sources. Providing sufficient spectral overlap of NC emission with dye absorption, excitation energy can be transferred from NCs to dye molecules labeled on secondary antibodies, thus confirming a binding effect. Large spectral distance between the emission of NCs and dye allows for easy resolution of both emission peaks, providing multiplexed detection. Figure 1b shows a typical fluorescence image of single NC-encoded microbeads obtained with this setup. The diameter of the excitation region was ~500 nm (insert in Figure 1b) allowing a scan over the surface of single microbeads and the measurement of emission spectra simultaneously. The fluorescence intensity statistically varied for different microbeads but was very similar (10% variation) for different scan areas of one and the same bead, indicating homogeneous distribution of NC within the presurface layer.

Figure 4c shows that the red emission from AlexaFluor633-labeled secondary antibody in solution can indeed be detected upon excitation by laser but not by the lamp. When the laser beam was focused on the surface of a single bead, both the orange emission from the NCs and the red emission from AlexaFluor633 have been detected (Figure 4d), confirming the presence of specifically bound AlexaFluor633-labeled secondary antibodies at the microbead's surface. The most interesting result was obtained with a NC-selective lamp excitation focused on a single bead. Here, both the orange emission from the NCs and the red emission from AlexaFluor633 were detected (Figure 4e), although the excitation by lamp falls beyond the dye absorption (Figure 4b), so that AlexaFluor633-labeled secondary antibodies in solution cannot be excited by lamp (Figure 4c). Hence, the NCs from the presurface layer of the microbeads effectively act as FRET donors for excitation of specifically bound AlexaFluor633-labeled secondary antibodies. Figure 4f shows the result of a control experiment, where no emission of AlexaFluor633 was detected under NC-tagged bead excitation by the lamp focused on a single microbead in the absence of topoI-specific antibody, where the binding of AlexaFluor633-labeled secondary antibody was not possible.

Measurements of fluorescence lifetime decays for aqueous suspensions of microbeads in the presence or absence of double-color immunocomplexes on their surface (Supporting Information) confirm the results of single-bead experiments. Fluorescence decay measured at the peak wavelength of the NC emission became faster when immunocomplex was formed (Figure 5), unambiguously indicating FRET from NCs to AlexaFluor633. The efficiency of the FRET process at the conditions of our experiment was limited to 25% for two reasons: small overlap of the emission spectrum of NCs with the absorption spectrum of AlexaFluor633 (Figure 4a) and the fact that the average distance between NCs in the presurface layer of the microbeads and the dye labels on the secondary antibodies in immunocomplexes can exceed the Förster radius of 56 Å previously reported for similar CdSe/ZnS NCs.[16,21] The 68 kDa fragment of topoI used for coating of microbeads has a typical crystal dimensions of 104 × 86 Å,[22] significantly exceeding the Förster radius. On the other hand, the thickness of the topoI layer in solution after its electrostatic adsorption on the bead's surface should be sufficiently smaller. In addition, a less-than-a-monolayer coverage of the microbead's surface with topoI is possible, which would facilitate a closer approach of AlexaFluor label to the NC-encoded bead's surface. Although the extent of a bead's surface coverage with topoI cannot be evaluated at this stage of the work, simple calculations show[23] that a reasonable average distance of 50 Å between AlexaFluor633 label and the NC-encoded bead's surface allows for efficiencies of FRET in the range of 25%, as we have observed.

The diameter of the excitation spot provided by our confocal microscope was ~500 nm (insert in Figure 1b). In the case of monolayer coverage of the microbead's surface with topoI molecules followed by formation of sandwich-like complexes (Figure 4a) with primary antibodies and dye-

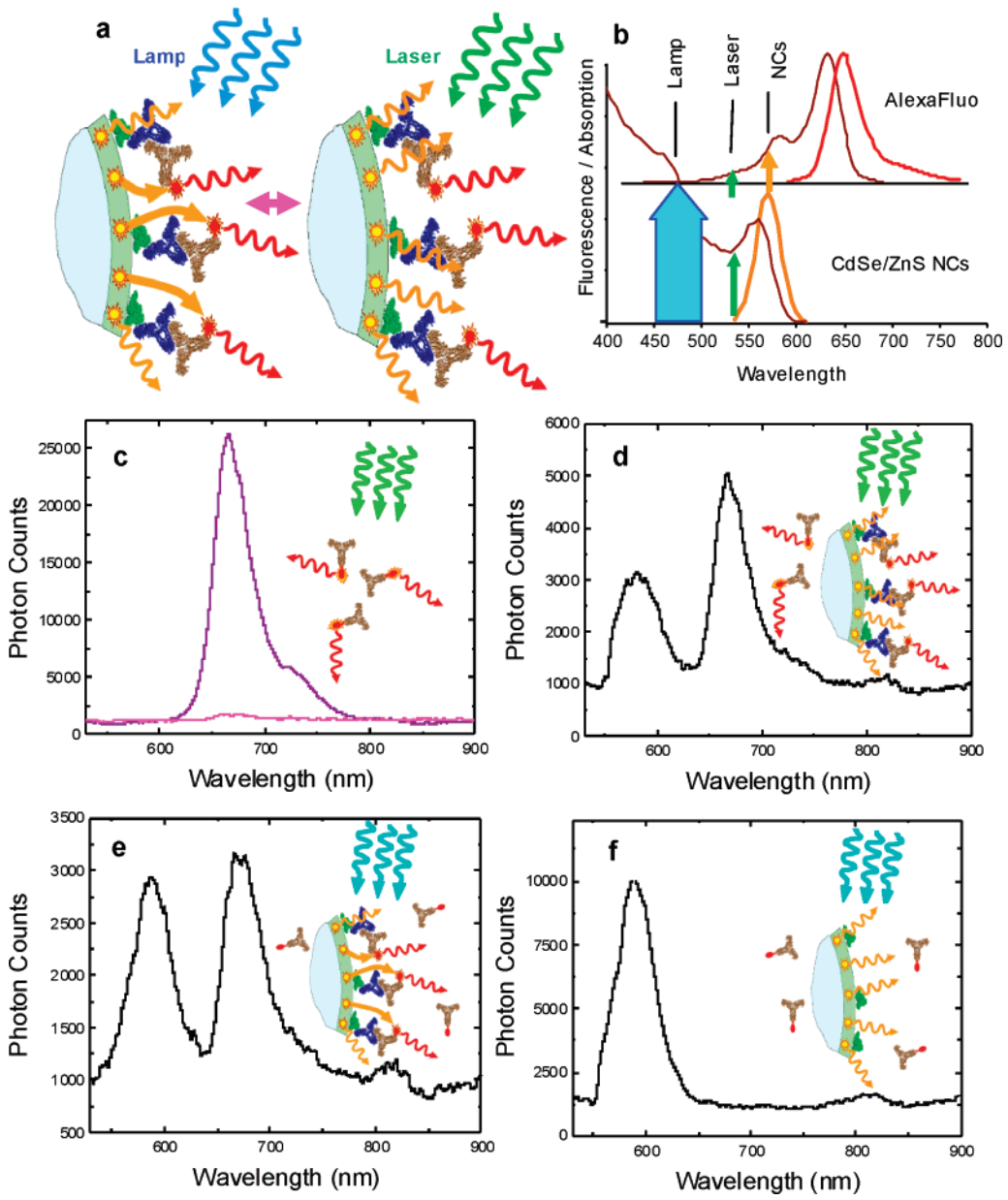

Figure 4. Single bead immunoassay for FRET detection of anti-topoisomerase I specific antibodies. (a) Scheme of a single bead FRET assay for immunodetection of anti-topoisomerase I antibodies, markers of systemic sclerosis, with NC-encoded, topoisomerase I-coated microbeads. Microbeads encoded with orange-emitting NCs and coated by 68 kDa recombinant fragment of topoI are incubated with anti-topoI specific monoclonal antibodies and stained with the AlexaFluor633-labeled secondary antibodies. Excitation is provided either by a 532 nm laser or by a 450−500 nm broad band lamp. (b) Absorption and emission spectra of CdSe/ZnS NCs and AlexaFluor633 dye. Excitation wavelengths for the laser (532 nm) and lamp sources (450−500 nm) are indicated. The lamp source selectively excites NCs but not the dye, while the laser source excites both NCs and dye. (c) Emission spectra measured from solution of AlexaFluor633-labeled secondary antibody under the laser (pink line) and lamp (red line) excitations. (d) Emission spectrum from a NC-encoded, topoI-coated microbead incubated with anti-topoI specific antibodies and stained with the AlexaFluor633-labeled secondary antibodies, *excitation by the laser*. (e) Emission spectrum from a NC-encoded, topoI-coated microbead incubated with the anti-topoI specific monoclonal antibodies and stained with the AlexaFluor633-labeled secondary antibodies, *excitation by the lamp*. (f) Negative control: No emission of AlexaFluor633 label on the secondary antibody is detected under the NC-selective *lamp excitation* focused on a single microbead in the absence of topoI-specific monoclonal primary antibody.

labeled secondary antibodies, a maximum of 30 complexes can be located within the fluorescence detection region on the microbead. We were, thus, able to detect fewer than 30 specifically bound antibodies with our setup. Selectively excited NCs transfer energy to the nearby antibody dye label allowing for detection of double-peak fingerprint emission with one peak originated from the NCs on the bead and another one from the dye label on the secondary antibody (Figure 4e). Specific interaction between the microbead and the antibody turns the fluorescence signal from dye label off and on (Figure 4e and Figure 4f), thus effectively discriminating between the occurrence and the nonoccurrence of the antibody binding effect. The absence of a fluorescent background from noninteracting with the beads dye-labeled

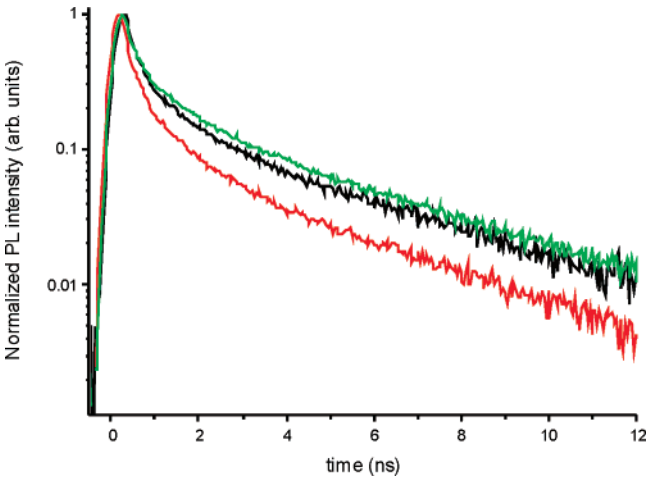

Figure 5. Fluorescence lifetime decay curves confirm energy transfer in two-color immunocomplexes of nanocrystal-encoded topoI-covered microbeads with anti-topoisomerase I antibodies and dye-labeled secondary antibodies. Fluorescence decay measured at the peak wavelength of the NC emission (570 nm) becomes faster for the two-color immunocomplexes (red line), as compared to solution of NCs-encoded, topoI-coated microbeads (black line) or to solution of NCs-encoded, topoI-coated microbeads stained with the AlexaFluor633-labeled secondary antibodies in the absence of topoI-specific antibodies (green line).

antibodies (Figure 4f) additionally increases the sensitivity of detection and further facilitates the multiplexing capabilities of immunodetection.

The autoantibodies are markers of diseases developing in healthy individuals,[24] and early discovery of minor amounts of candidate autoantigens becomes essential for diagnose and treatment of autoimmune diseases.[25,26] Planar surface arrays currently offer the greatest per-array complexities but are limited by their methods of binding autoantigens and suffer from drying which can distort and/or sterically interfere with immunologic epitopes.[26] Liquid-phase microbead-based assays utilizing minimally disruptive methods to label antigens are free from these limitations.[25] Our results will open the way to NC-based clinical assays with previously unachievable detection sensitivity. High-throughput screening utilizing unique and robust fluorescence properties of NC-encoded beads will enable effective determination of multiple autoantibodies and enhance the clinical sensitivity and specificity of autoantibody screening for ultrasensitive multiplexed diagnostics.

Acknowledgment. I.N. and A.S. thank financial support from NATO Collaborative Linkage Grants and INTAS Innovation Programs. A.S. is grateful to FEBS for providing a long-term fellowship and follow-up funds. V.O. acknowledges partial support from INTAS and RFBR Grants 06-04-48373, 07-04-12081, and 06-02-17036. The Munich team was supported by the Excellence Cluster NIM of the DFG; A.S.S. and A.L.R. acknowledge support from the Volkswagen Foundation (Grant I/80 052). I.N. acknowledges partial support from ANR program.

Supporting Information Available: Descriptions of experimental conditions including synthesis and water solubilization of nanocrystals, preparation of microbeads encoded with fluorescent nanocrystals, production of catalytically active 68 kDa fragment of recombinant human DNA-topoisomerase I, coating of NC-encoded fluorescent beads with 68 kDa recombinant fragment of human DNA-topoisomerase I, immunoassays, preparation of NC-encoded microbeads covered by Sm-antigen and nRNP complex, fluorescence measurements on single microbeads, and time-resolved measurements on NC-encoded microbeads in suspensions, a table of typical statistics of fluorescence responses generated by monoclonal anti-topoisomerase I, and figures showing expression, purification, and characterization of 68 kDa recombinant fragment of human DNA topoisomerase I and cleavage of "suicide oligonucleotide" with recombinant 68 kDa fragment of human DNA topoisomerase I. This material is available free of charge via the Internet at http://pubs.acs.org.

References

(1) Hueber, W.; Utz, P. J.; Steinman, L.; Robinson, W. H. *Arthritis Res.* **2002**, *4*, 290.
(2) Douvas, A. S.; Achten, M.; Tan, E. M. *J. Biol. Chem.* **1979**, *254*, 10514.
(3) Shero, J. H.; Bordwell, B.; Rothfield, N. F.; Earnshaw, W. C. *Science* **1986**, *231*, 737.
(4) Pollock, W.; et al. *J. Clin. Pathol.* **2002**, *55*, 680.
(5) Ulvestad, E.; et al. *Scand. J. Immunol.* **2000**, *52*, 309.
(6) Westman, K. W.; et al. *Kidney Int.* **1998**, *53*, 1230.
(7) Lal, G.; et al. *J. Immunol. Methods* **2005**, *296*, 135.
(8) Braeckmans, K.; De Smedt, S. C.; Leblans, M.; Pauwels, R.; Demeester, J. *Nat. Rev. Drug Discovery* **2002**, *1*, 447.
(9) Braeckmans, K.; et al. *Nat. Mat.* **2003**, *2*, 169.
(10) Robinson, W. H.; et al. *Nat. Med.* **2002**, *8*, 295.
(11) Naciff, J. M.; et al. *Environ. Health Perspect.* **2005**, *113*, 1164.
(12) Martins, T. B.; et al. *Clin. Diagn. Lab. Immunol.* **2004**, *11*, 1054.
(13) Han, M.; Gao, X.; Su, J. Z.; Nie, S. *Nat. Biotechnol.* **2001**, *19*, 631.
(14) Xu, H.; et al. *Nucl. Acid Res.* **2003**, *31*, e43.
(15) Eastman, P. S.; Ruan, W.; Doctolero, M.; Nuttall, R.; de Feo, G.; Park, J. S.; Chu, J. S. F.; Cooke, P.; Gray, J. W.; Li, S.; Chen, F. F. *Nano Lett.* **2006**, *6*, 1059.
(16) Medintz, I. L.; et al. *Nat. Mater.* **2003**, *2*, 630.
(17) Sukhanova, A.; et al. *Lab. Invest.* **2002**, *82*, 1259.
(18) Wargnier, R.; Baranov, A. V.; Maslov, V. G.; Stsiapura, V.; Artemyev, M.; Pluot, M.; Sukhanova, A.; Nabiev, I. *Nano Lett.* **2004**, *4*, 451.
(19) Caruso, F. *Adv. Mater.* **2001**, *13*, 11.
(20) Susha, A. S.; et al. *Colloids Surf., A* **2000**, *163*, 39.
(21) Medintz, I. L.; Uyeda, H. T.; Goldman, E. R.; Mattoussi, H. *Nat. Mater.* **2005**, *4*, 435.
(22) Redinbo, M. R, Champoux, J. J.; Hol, W. G. *Biochemistry* **2000**, *39*, 6832.
(23) Nikiforov, T. T.; Beechem, J. M. *Anal. Biochem.* **2006**, *357*, 68.
(24) Scofield, R. H. *Lancet* **2004**, *363*, 1544.
(25) Craighead, H. *Nature* **2006**, *442*, 387.
(26) Conzàlez-Buitrago, J. M.; Gonzàlez, C. *Clin. Chim. Acta* **2006**, *365*, 50.

NL070966+